Compositional Variations in Smectites: Part I. Alteration of Intermediate Volcanic Rocks. A Case Study from Milos Island, Greece

2 AUTHORS, INCLUDING:

G.E. Christidis
Technical University of Crete

48 PUBLICATIONS   **690** CITATIONS

COMPOSITIONAL VARIATIONS IN SMECTITES: PART I. ALTERATION OF INTERMEDIATE VOLCANIC ROCKS. A CASE STUDY FROM MILOS ISLAND, GREECE

G. CHRISTIDIS AND A. C. DUNHAM

Department of Geology, University of Leicester, University Road, Leicester LE1 7RH, UK

ABSTRACT: The chemistry of smectites from some bentonite deposits derived from intermediate rocks has been examined by electron microprobe methods. A large variation in chemical composition within very short distances, principally controlled by a well-defined negative relationship between Si and Al, and between Al^{VI} and Fe^{3+} and Al^{VI} and Mg has been observed. On the other hand, Mg does not vary systematically with either Si or Fe^{3+}. In several bentonites beidellite coexists with montmorillonite and there is a compositional transition between the two smectite minerals, implying the existence of a possible solid-solution series. This transition occurs only when Cheto-type montmorillonites are present, being absent for Wyoming-type montmorillonites. No compositional transition between Wyoming- and Cheto-type montmorillonite was observed. It is believed that the compositional variations reflect initial chemical gradients originated during the devitrification of the volcanic glass, due to the migration of chemical components.

The heterogeneity of smectites, both structural and chemical, has been investigated extensively. Using X-ray diffraction methods, Byrne (1954), McAtee (1958b), and Tettenhorst & Johns (1966) found that montmorillonites constitute mixed-layer sequences which exhibit random interstratification. McAtee (1958a) proposed that montmorillonites are composed of two separate phases, one Na-rich and one Ca-rich. Applying alkylammonium treatments, Stul & Mortier (1974), Lagaly & Weiss (1975), Lagaly *et al.* (1976) and Lagaly (1981) determined that smectites are heterogeneous having an inhomogeneous distribution of layer charge in their structure. However, this analytical method cannot locate the source of the layer charge within the structure and consequently the source of the heterogeneous charge distribution (Lagaly *et al.*, 1976). Goulding & Talibudeen (1980) and Talibudeen & Goulding (1983) showed that there is heterogeneity in the exchangeable sites of smectites, which are not thermodynamically equivalent, contributing to variable layer expansion, a property of smectites well known from the work of Norrish (1954). Also, Goodman *et al.* (1988) using Mössbauer and EPR spectroscopy showed that the bentonites they studied could be separated into at least two smectite populations on the basis of different Fe content. Nadeau *et al.* (1985) found that the Unterrupsroth beidellite is a mixture of materials varying from more beidellitic to more montmorillonitic in character. Lim & Jackson (1986) reported the existence of random interstratification of montmorillonite with some beidellite layers in several bentonites and soil smectitic clays.

Based mainly on differences in their thermal and chemical properties, Grim & Kulbicki (1961) proposed that Al-rich montmorillonites are a mixture of two types: Wyoming and

Cheto which are separate and do not form any kind of solid-solution. Weaver & Pollard (1973) agreed with this division. Schultz (1969) further subdivided the Cheto type into the Tatatilla, Otay and Chambers types. This classification scheme was essentially retained by Brigatti & Poppi (1981) and is generally accepted (Newman & Brown, 1987, Güven 1988), although Alberti & Brigatti (1985) questioned the existence of separation between Chambers and Otay types.

Most of the main sources of information about chemical variations of smectites are based on chemical analyses of the bulk clay fraction or sub-fractions. Consequently, they represent an average value of the chemical parameters examined. More recently, electron beam techniques have revealed greater details about the heterogeneity of smectites, although analyses have been limited and commonly averaged (Ramseyer & Boles 1986; Bouchet *et al.*, 1988; Altaner & Grim, 1990; Singh & Gilkes, 1991). Banfield & Eggleton (1990) studying the weathering products of muscovite and feldspars, found substantial variation in the chemistry of the smectites formed, using a limited number of microanalyses.

As far as the authors can establish, there is still insufficient information published about either the extent and limits within which the chemical heterogeneity in a smectitic material varies, or the source of the heterogeneity of the layer charge. Therefore, this paper has three aims: (a) to describe the chemical aspects of the heterogeneity of smectites from Milos island; (b) to investigate the coexistence of different types of smectites and the possibility of existence of any solid-solution series between them; and (c) to discuss the possible chemical factors which control the genesis of smectites. The materials come from andesitic and dacitic volcanic precursors. In a second contribution, bentonites derived from acid rocks will be presented.

GEOLOGICAL SETTING

Geology of Milos island

The island of Milos is situated in the SW part of the South Aegean Volcanic Arc (Fig. 1a), which was created from the subduction of the African Plate under the deformed margin of the Eurasian Plate (Fyticas *et al.*, 1986). Sonder (1924), and Fyticas (1977) studied the geological framework of the island and distinguished (Fig. 1b): (i) An Alpine metamorphic basement characterized by an Middle Eocene high pressure/low temperature metamorphic event overprinted by a high temperature/low pressure one at the boundary between Oligocene and Miocene (Kornprobst *et al.*, 1979; Hoffman & Keller, 1979). K-Ar and Rb-Sr determinations (Altherr *et al.*, 1979) give 45 ± 5 Ma for the first and 25 ± 5 for the second event. (ii) A Neogene marine sedimentary sequence of Upper Miocene age (Fyticasi, 1977). (iii) A volcanic sequence, the product of eruptive activity which started in the Upper Pliocene (Fyticas *et al.*, 1976, 1986; Angelier *et al.*, 1977) and produced both pyroclastics and lavas, the composition of which varies from rhyolites to low-Si andesites (Fyticas, 1977; Fyticas *et al.*, 1986). The volcanic activity, which occurred under both subaerial and submarine conditions, started in the western part of the island and migrated to the eastern part in the Lower Quaternary (Fyticas *et al.*, 1986). Subsequent alteration of these volcanics gave rise to extensive bentonite deposits in the eastern part and small kaolin deposits mainly in the western part of the island. (iv) Alluvial deposits.
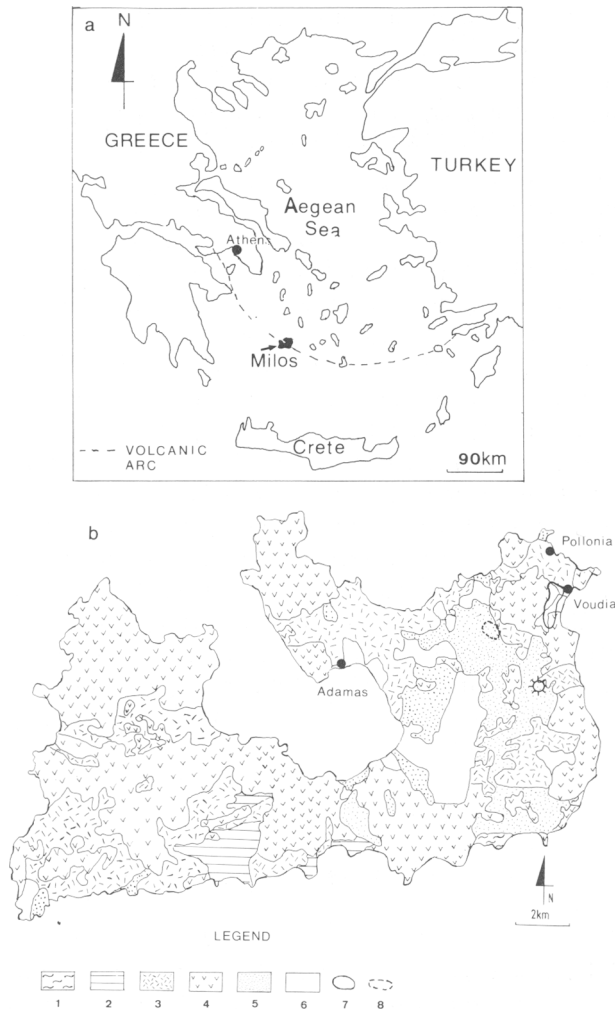
FIG. 1. a: Location of Milos Island. b: Simplified geological map of Milos Island, modified after Fyticas *et al.* (1986). 1 = metamorphic basement; 2 = Neogene sedimentary sequence; 3 = pyroclastic rocks; 4 = undifferentiated lavas; 5 = Chaotic formation described as "green lahar" by Fyticas (1977); 6 = alluvial deposits; 7 = location of area 1; 8 = location of area 2.

Geology of the bentonite deposits

The bentonite deposits of eastern Milos have developed mainly at the expense of volcaniclastic rocks and, to a lesser extent, of lavas which vary in composition from andesitic to rhyodacitic-rhyolitic. The parent materials were emplaced under marine conditions, but it is not clear whether the alteration was mainly devitrification of the original glass (Wetzenstein, 1969, 1972), or hydrothermal (Fyticas, 1977) or both (Luttig & Wiedenbein, 1990). The deposits form massive stratiform bodies having thicknesses well in excess of 30 m at several sites. Their contact with the overlying rocks is abrupt. Their base is not known with certainty being revealed only at one site where the bentonite lies

unconformably on the metamorphic basement. Several deposits, especially those derived from acid precursors, are rich in opal C-T which is either thoroughly distributed throughout the bentonite mass or forms separate beds showing no systematic distribution in the bentonite horizons.

MATERIALS AND METHODS

Eight bentonite samples collected from the deposits of Aspro Horio, Tsantili, Zoulias, Ankeria and Koufi, located in the NE part of Milos (Fig. 1b) were examined (Table 1). The first three deposits are located in area 1 while the rest are in area 2 (Fig. 1b). Samples SM99, SM114, SM119, and SM228 belong to the same bentonite horizon, as do SM25 and SM43.

All samples were examined by X-ray diffraction (XRD) for bulk mineralogy using a Philips powder diffractometer equipped with a PW1710 fully computerized control unit, operating at 40 kV and 30 mA, using Ni-filtered Cu-$K\alpha$ radiation. Scanning speed was $1°\ 2\theta$/min. Clay mineralogy was determined by sedimentation methods after dispersion in distilled water using ultrasonic vibration. Sodium polymetaphosphate was used as deflocculant, so it is assumed that at least partial Na-exchange occurred. The $<2\ \mu m$ fraction was separated, spread on glass slides and allowed to dry in atmospheric conditions. The slides were then saturated with ethylene glycol at 60°C for at least 16 h to ensure maximum saturation.

Epoxy impregnated polished blocks of the samples were analysed with a JEOL JXA-8600 Superprobe, equipped with three wavelength dispersive spectrometers (WDS) and a Link series 1 energy dispersive spectrometer (EDS), with 158 eV resolution at 5·8 KeV. Analyses were carried out with the EDS using 100 s livetime, 15 kV acceleration current potential, and 3 nA sample current. A 5 μm diameter (defocused) beam was used. The use of back-scattered electron images enabled distinction of smectites from contaminants like Ti oxides, Fe oxides and sulphides. All selected points were analysed for Si, Ti, Al, Fe, Mn, Mg, Ca, Na, and K. A minimum of 20 points were chosen from each sample and 300 points

TABLE 1. Mineralogical composition of the bentonites studied based on XRD results.

| | Area 1 | | | | Area 2 (Samples SM25 ans SM43 from the same bentonite horizon) | | | |
| | (All samples from the same bentonite horizon) | | | | | | | |
	Tsantili deposit	Aspro Horio deposit		Zoulias deposit	Ankeria deposit		Koufi depostit	
Minerals	SM99	SM114	SM119	SM228	SM16	SM25	SM43	SM66
Smectite	M	M	M	M	M	M	M	M
Kaolinite	T	–	–	–	–	–	–	T
K-feldspar	A	–	A	–	–	T	–	A
Plagioclase	–	P	A	–	–	A	A	–
Opal-CT	–	P	–	–	–	A	–	–
Quartz	A	A	A	A	–	–	–	–
Calcite	A	–	–	–	–	A	–	–
Siderite	T	–	–	–	–	–	–	–
Halite	T	–	–	–	–	–	–	–
Pyrite	T	T	T	–	–	T	T	T

M = major mineral phase; A = abundant phase; T = trace phase.

analysed. Measured concentrations were automatically corrected for atomic number, absorption in the sample, fluorescence, and dead time (the ZAF correction) using the ZAF-4 computer program provided by Link. The following standards were used: wollastonite for Si and Ca, jadeite (intensity standard) and NaCl (profile standard) for Na, synthetic Al_2O_3 for Al, synthetic MgO for Mg, microcline for K, synthetic Fe_3O_4 for Fe, rutile for Ti and rhodonite for Mn. Cobalt was used as a secondary standard to monitor the overall count rates.

The accuracy, precision and detection limits of the method have been examined by Dunham & Wilkinson (1978). Titanium, when detected, was always associated with Ti oxides and consequently was always subtracted from the total. Manganese was always below the detection limit of the instrument. The totals obtained varied between 71 and 94%. Similar totals have been reported (Ramseyer & Boles, 1986) and have been attributed mainly to variations in the water content of smectites, to the existence of microporosity between the clay particles (Ramseyer & Boles, 1986) and to possible volatilization of alkalies especially Na, which is usually present in small quantities and consequently is easily lost (Velde, 1984).

The structural formulae were obtained using 11 oxygens with the following assignments: the empty sites in the tetrahedral positions were filled with Al to make Si + Al = 2. The remaining Al was assigned to octahedral sites. Iron was assumed to be entirely ferric and all Mg was assigned to octahedral positions. Calcium, Na, and K were assigned to exchangeable positions.

RESULTS

X-ray diffraction data

The XRD results for the bulk samples are presented in Table 1. In all samples dioctahedral smectite is the main mineral phase, associated with K-feldspar, plagioclase and a silica phase, either quartz or opal C-T, or both. The structural state of K-feldspar was determined as high-sanidine, using the criteria of Wright (1968). Pyrite occurs in small amounts in all samples. Calcite and ankerite are present in samples SM25 and SM99, respectively. Kaolinite is present in small amounts in SM66 and SM99. Representative XRD traces of the bulk samples are shown in Fig. 2a.

The XRD results for the clay fractions (Fig. 2b) show that smectite is the principal clay mineral phase present, with subordinate kaolinite in samples SM66 and SM99, confirming the results for the bulk samples.

Microprobe results

Average values, standard deviations, and minimum and maximum values of the elements analysed and the cation distributions are presented in Table 2. The results show a large chemical, and consequently structural, variation between smectite crystals within the same sample.

The substitution of Fe^{3+} for Al in the octahedral sites varies widely providing an almost perfect negative relationship between them (Fig. 3a,b,c). A similar relationship (not shown here) exists also between total Al and Fe^{3+}. Such a relationship, although expected, has not so far been reported. On the contrary, Grim & Güven (1978) and Güven (1988) reported the lack of any relationship between these two elements while Weaver & Pollard (1973)
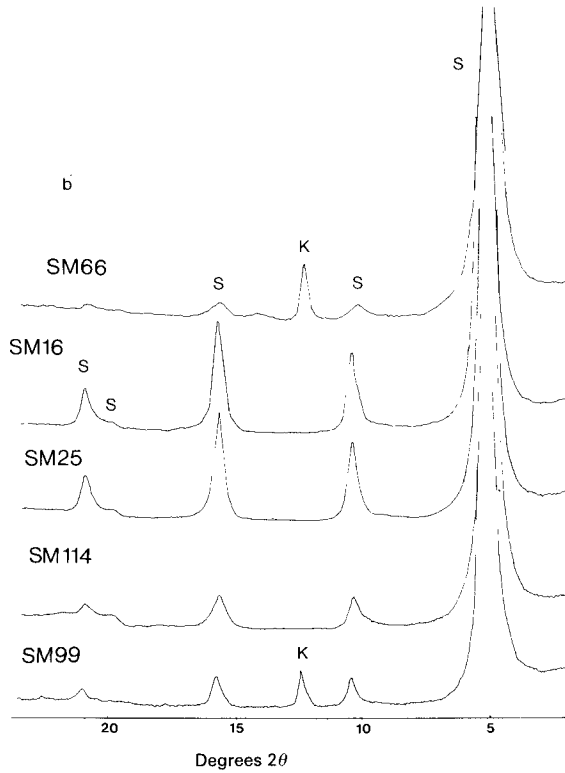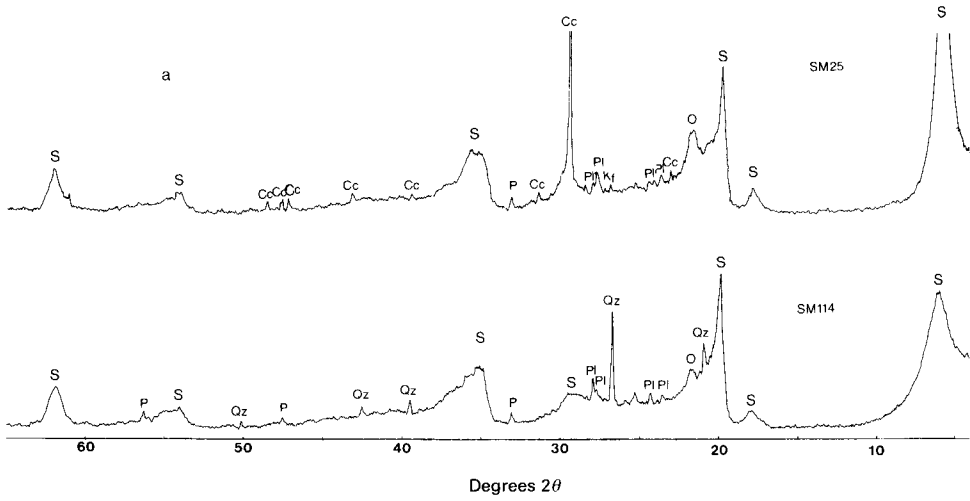
FIG. 2. Representative XRD traces of the Greek bentonites studied: (a) bulk sample; (b) <2 μm clay fractions. S = smectite, K = kaolinite, Qz = quartz, Pl = plagioclase, Kf = K-feldspar, O = opal C-T, Cc = calcite, P = pyrite. Cu-$K\alpha$ radiation.

TABLE 2. Microanalyses (wt%) and structural formulae of smectites.

Sample	SM16 (n = 28)				SM25 (n = 33)			
	mean	sd	max	min	mean	sd	max	min
SiO_2	54·81	2·46	59·72	49·27	56·78	1·89	60·66	52·69
Al_2O_3	20·28	1·54	23·00	17·41	21·17	2·41	25·14	16·93
Fe_2O_3	2·89	1·63	5·41	0·52	3·06	1·84	5·97	0·88
MgO	4·09	0·46	5·18	3·08	3·78	0·66	4·99	2·64
CaO	1·67	0·40	3·49	1·26	1·91	0·29	2·58	1·47
Na_2O	0·58	0·15	0·90	0·41	0·49	0·09	0·81	0·43
K_2O	0·61	0·55	2·47	0·21	0·48	0·61	2·43	0·22
Total	84·63	–	–	–	87·14	–	–	–

Structural formulae based on 11 Oxygens
Tetrahedral cations

	mean	sd	max	min	mean	sd	max	min
Si	3·83	0·03	3·89	3·75	3·58	0·05	3·95	3·74
Al^{IV}	0·17	0·03	0·25	0·11	0·15	0·05	0·26	0·05

Octahedral cations

	mean	sd	max	min	mean	sd	max	min
Al^{VI}	1·50	0·09	1·68	1·37	1·53	0·14	1·73	1·30
Fe^{3+}	0·15	0·09	0·29	0·03	0·16	0·09	0·33	0·04
Mg	0·42	0·03	0·50	0·36	0·38	0·06	0·48	0·26
VICations	2·08	0·03	2·12	1·99	2·07	0·03	2·14	2·00

Interlayer cations

	mean	sd	max	min	mean	sd	max	min
Ca	0·13	0·03	0·26	0·09	0·14	0·02	0·20	0·11
Na	0·07	0·02	0·12	0·00	0·03	0·03	0·10	0·00
K	0·03	0·05	0·25	0·00	0·01	0·04	0·21	0·00
Layer Charge	0·35	0·08	0·65	0·23	0·32	0·07	0·47	0·22
Inter. Charge	0·35	0·08	0·65	0·23	0·32	0·07	0·47	0·22

Sample	SM43 (n = 37)				SM66 (n = 43)			
	mean	sd	max	min	mean	sd	max	min
SiO_2	57·06	2·14	60·85	52·55	52·21	3·37	57·87	41·75
Al_2O_3	20·83	3·24	27·17	16·43	20·89	3·79	27·87	16·49
Fe_2O_3	4·55	2·51	10·07	1·30	2·38	1·15	4·06	0·50
MgO	3·39	0·94	5·47	1·44	3·01	0·78	4·21	1·03
CaO	1·49	0·26	2·43	1·12	0·75	0·18	1·17	0·31
Na_2O	0·68	0·31	1·58	0·41	0·62	0·17	0·98	0·42
K_2O	0·54	0·27	1·14	0·23	0·76	0·39	1·75	0·26
Total	88·17	–	–	–	80·38	–	–	–

Structural formulae based on 11 Oxygens
Tetrahedral cations

	mean	sd	max	min	mean	sd	max	min
Si	3·84	0·08	3·98	3·65	3·82	0·17	4·08	3·36
Al^{IV}	0·16	0·08	0·35	0·02	0·18	0·17	0·64	−0·08

Octahedral cations

	mean	sd	max	min	mean	sd	max	min
Al^{VI}	1·50	0·19	1·78	1·16	1·63	0·17	2·01	1·43
Fe^{3+}	0·23	0·12	0·49	0·07	0·13	0·06	0·22	0·03
Mg	0·34	0·10	0·56	0·15	0·33	0·09	0·45	0·12
VICations	2·06	0·04	2·12	1·90	2·09	0·05	2·21	1·98

Interlayer cations

	mean	sd	max	min	mean	sd	max	min
Ca	0·11	0·02	0·18	0·08	0·06	0·01	0·09	0·03
Na	0·07	0·05	0·21	0·00	0·06	0·05	0·13	0·00
K	0·02	0·03	0·09	0·00	0·07	0·04	0·16	0·00
Layer Charge	0·31	0·09	0·61	0·18	0·24	0·07	0·40	0·13
Inter. Charge	0·31	0·09	0·61	0·18	0·24	0·07	0·40	0·13

TABLE 2. *Continued.*

Sample	SM99 (n = 39)				SM114 (n = 22)			
	mean	sd	max	min	mean	sd	max	min
SiO_2	54·10	1·23	56·56	51·18	47·03	1·55	50·17	44·35
Al_2O_3	18·09	1·38	22·48	16·38	14·71	0·96	16·49	13·11
Fe_2O_3	3·20	0·83	4·81	1·62	4·26	0·86	5·87	2·81
MgO	3·23	0·28	3·92	2·71	3·04	0·29	3·86	2·54
CaO	1·54	0·21	1·94	0·88	1·26	0·18	1·58	0·86
Na_2O	0·29	0·25	0·67	0·00	0·51	0·24	0·84	0·00
K_2O	0·40	0·33	1·46	0·00	0·41	0·45	2·24	0·00
Total	80·84	–	–	–	71·22	–	–	–
Structural formulae based on 11 Oxygens								
Tetrahedral cations								
Si	3·95	0·05	4·01	3·81	3·93	0·04	3·98	3·82
Al^{IV}	0·05	0·05	0·19	−0·01	0·07	0·04	0·18	0·02
Octahedral cations								
Al^{VI}	1·50	0·06	1·66	1·38	1·38	0·08	1·50	1·21
Fe^{3+}	0·18	0·05	0·28	0·09	0·27	0·06	0·38	0·19
Mg	0·35	0·03	0·41	0·29	0·38	0·03	0·50	0·33
VICations	2·03	0·02	2·08	1·98	2·03	0·02	2·09	1·99
Interlayer cations								
Ca	0·12	0·02	0·15	0·07	0·11	0·01	0·13	0·08
Na	0·04	0·04	0·10	0·00	0·08	0·04	0·14	0·00
K	0·04	0·03	0·14	0·00	0·04	0·05	0·25	0·00
Layer Charge	0·32	0·05	0·45	0·23	0·35	0·05	0·44	0·28
Inter. Charge	0·32	0·05	0·45	0·23	0·35	0·05	0·44	0·28

Sample	SN119 (n = 34)				SM228 (n = 21)			
	mean	sd	max	min	mean	sd	max	min
SiO_2	55·26	2·99	61·03	50·46	56·25	1·72	59·06	52·58
Al_2O_3	18·92	1·15	21·31	16·49	19·71	1·92	23·04	16·58
Fe_2O_3	3·72	1·47	6·47	1·44	4·28	1·83	7·01	1·29
MgO	3·36	0·52	5·32	2·25	4·32	0·31	4·84	3·97
CaO	1·12	0·19	1·44	0·45	1·09	0·15	1·34	0·71
Na_2O	0·64	0·26	1·39	0·00	0·55	0·22	0·86	0·00
K_2O	0·47	0·65	2·27	0·00	0·08	0·14	0·43	0·00
Total	83·50	–	–	–	86·28	–	–	–
Structural formulae based on 11 Oxygens								
Tetrahedral cations								
Si	3·91	0·05	3·98	3·68	3·68	0·05	3·93	3·76
Al^{IV}	0·09	0·05	0·32	0·02	0·14	0·05	0·24	0·07
Octahedral Cations								
Al^{IV}	1·49	0·09	1·63	1·30	1·45	0·10	1·62	1·31
Fe^{3+}	0·20	0·07	0·34	0·08	0·22	0·09	0·35	0·07
Mg	0·35	0·05	0·53	0·26	0·44	0·02	0·48	0·40
VICations	2·05	0·03	2·14	1·97	2·11	0·02	2·15	2·08
Interlayer cations								
Ca	0·09	0·02	0·11	0·04	0·08	0·01	0·09	0·05
Na	0·09	0·03	0·20	0·00	0·07	0·03	0·11	0·00
K	0·04	0·06	0·22	0·00	0·01	0·01	0·04	0·00
Layer Charge	0·30	0·08	0·56	0·16	0·24	0·03	0·29	0·16
Inter. Charge	0·30	0·08	0·56	0·16	0·24	0·03	0·29	0·16

n = number of analyses per sample; sd = standard deviation; min = minimum value; max = maximum value.

found a weak negative relationship ($r = -0.56$). A negative relationship is observed also between Al and Mg (Fig. 3d,e,f), in accordance with the data provided by Grim & Güven (1978), Güven (1988) and Weaver & Pollard (1973). In area 1 it seems that smectites from sample SM228 (Zoulias Quarry) do not follow the general trend but display a rather constant Mg content over a range of Al^{VI} values. Although the relationship between Al^{VI} and both Fe^{3+} and Mg has the same characteristics in all smectites examined, the slope of the correlation is different for samples from different horizons.

The relationship between Mg and Si does not have a constant pattern in the different areas (Fig. 4a,b,c). They display a clear, although relatively weak, positive relationship in area 2, except for sample SM16, where no particular relationship is observed, and a lack of any relationship in area 1. Smectites from sample SM228 (area 1) show a different behaviour having a good negative relationship between Mg and Si. It seems, therefore, that in area 2, decrease of the tetrahedral charge is accompanied by an increase in octahedral charge, confirming the assumption of Weaver & Pollard (1973). However, this is not the case in area 1, especially in Zoulias quarry (sample SM228) where the opposite trend is implied. A similar lack of a particular trend for smectites from the two areas is observed between Fe^{3+} and Si (Fig. 4d,e,f). A positive trend is observed in area 2 but there is no particular relationship in area 1. An exception to these trends is displayed by sample SM228 (area 1) for which a weak positive trend is visible, and by sample SM16 where Fe^{3+} varies over a long range, with Si remaining essentially constant.

An interesting positive trend is displayed by Fe^{3+} and Mg for the smectites in the samples of area 1 (Fig. 5a,b,c) although Weaver & Pollard (1973) determined a weak negative relationship for these elements. Smectites from SM228 follow a different trend characterized by a weak negative relationship. This implies that an increase in the substitution of Fe for Al is associated with an increase in octahedral charge. On the other hand, in SM228, substitution of Fe for Al seems to favour a decrease of octahedral charge. No particular trend is observed in smectites from area 2, except those from sample SM66 which exhibit a good positive relationship complying with the overall trend displayed by smectites in area 1.

Total Al and Si have the expected negative relationship which is very well displayed in area 2 (Fig. 5d,e,f). In area 1 the greater scatter is mainly due to smectites from sample SM99 which have higher Si contents; this is considered to be the result of a secondary extensive illitization process due to hydrothermal alteration in this quarry, leading to a release of Si from the illitized smectites (Christidis, unpublished data).

The effect of different octahedral cation occupancy in the structural formulae of smectites is depicted in the "smectite triangle" (Fig. 6), the three apices of which are occupied by the octahedral cations (Güven, 1988). It can be seen that the smectite population in each sample: (a) does not fall in a single "field" assigned for a particular type, implying coexistence of different smectite types, and (b) shows clear compositional trends which are more or less representative for the whole area it comes from. For instance, smectites from area 1 plot in the field of the Wyoming-type montmorillonite and in an area between the fields of Wyoming and Fe-rich montmorillonite, while those of area 2 are in the field occupied by beidellite and Cheto-type (Grim & Kulbicki's definition). An exception to the trend shown by area 1 is sample SM228 which does not display the continuous variation observed, but seems to be composed of two distinct populations; one which follows the overall trend of this horizon, and a second which plots in the field of Cheto-type montmorillonites. In addition, in area 2 it is observed that the smectites from sample SM43
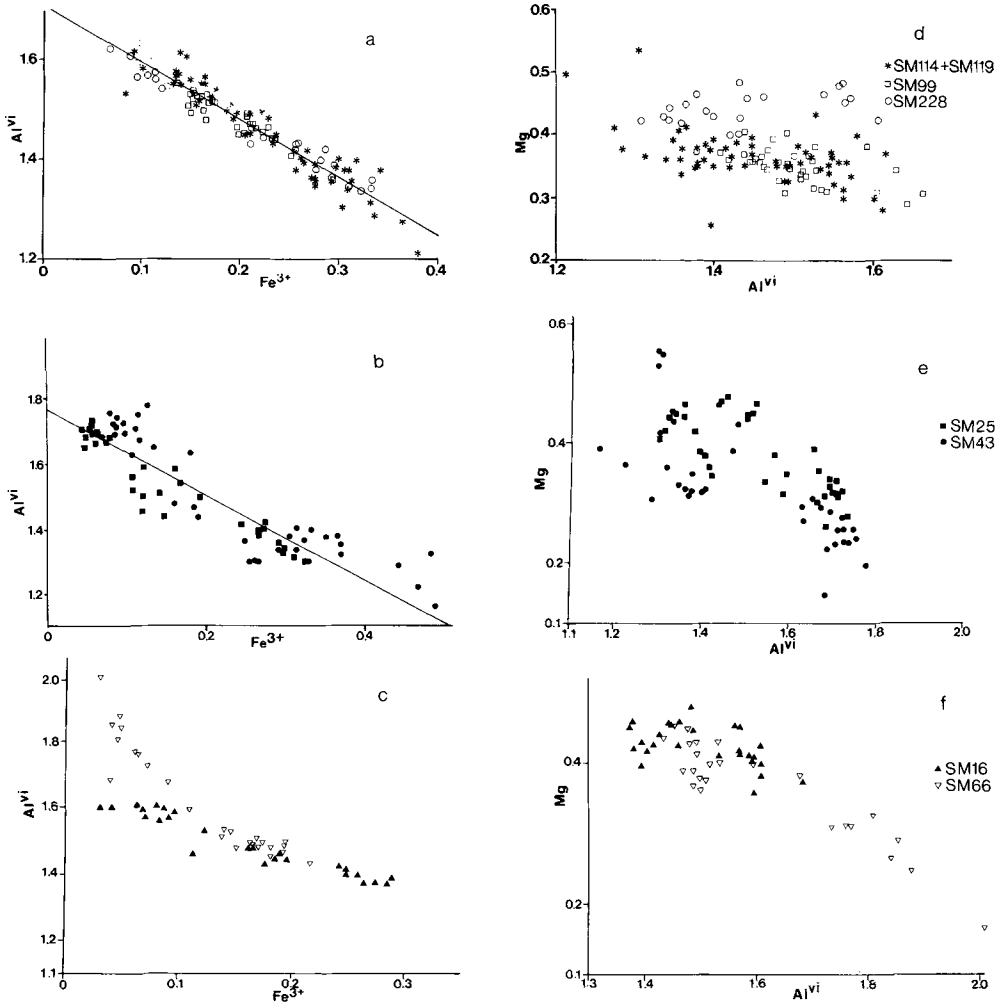
Fig. 3. Relationship between Al^{VI} and the other octahedral cations. Note the well expressed negative relationship between octahedral Al and both Fe and Mg, and the different slopes of the lines in the different areas. See text for discussion of the trends observed. Symbols for a, b and c are the same as for d, e and f.

always have a higher Fe^{3+} content than their counterparts from sample SM25. In both areas a continuous variation is observed and it seems that both series converge in an area close to the Fe-montmorillonite "field". Although there seems to be a continuous compositional transition from beidellite to Fe-montmorillonite through Cheto-type montmorillonite, such a trend is not observed when Wyoming montmorillonites are present. Such a coexistence between beidellite and montmorillonite has been reported by Lim & Jackson (1986) and Yamada *et al.* (1991).

Similar compositional transitions, although not so clear, are also observed when smectites are plotted in the triangular diagram having MR^3-$2R^3$-$3R^2$ coordinates (Fig. 7),
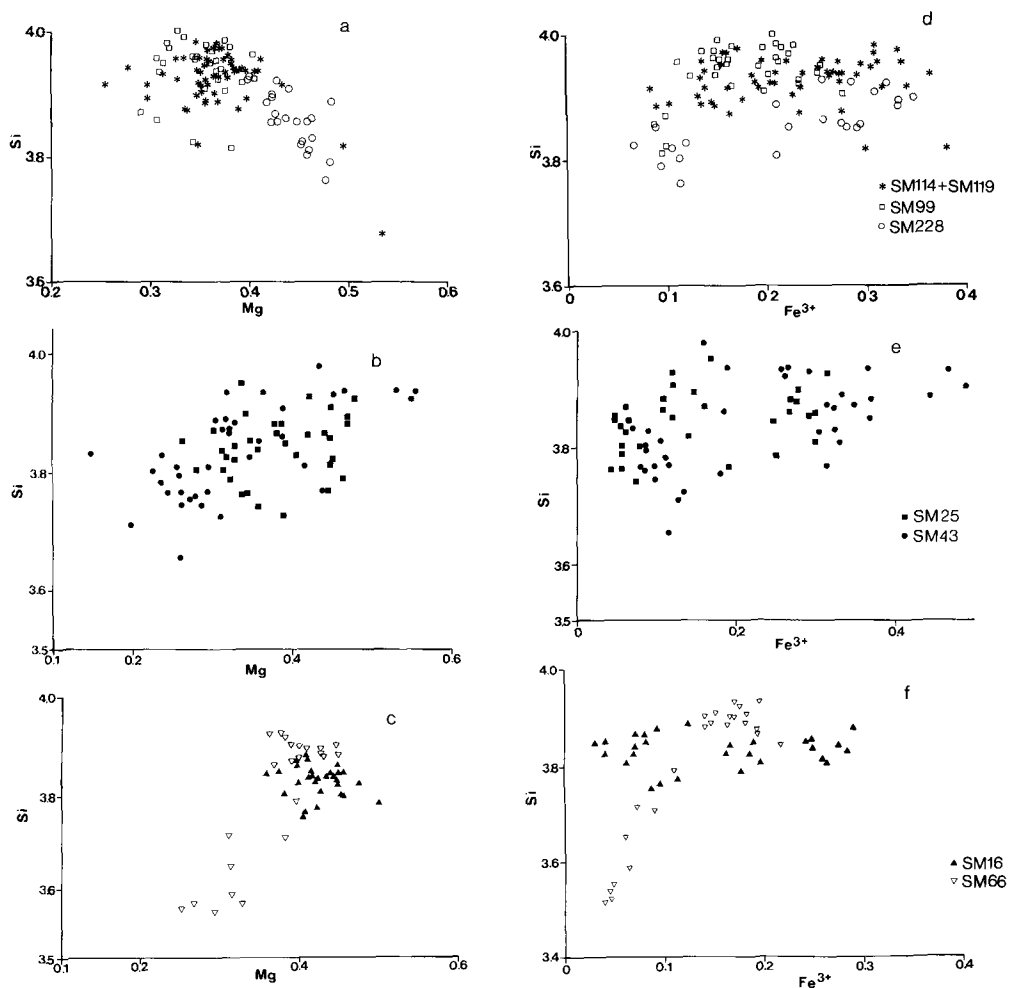
FIG. 4. Si *vs.* Mg (a–c) and Si *vs.* Fe^{3+} (d–f) in smectites from different areas. See text for discussion about the trends observed. Symbols for a, b and c are the same as for d, e and f.

using the cation assignments proposed by Velde (1985). Smectites from area 1 display the same trends in their compositional variation and are plotted within the "field" of fully expandable smectites. They develop variation mainly along the $2R^3$-MR^3 direction having a more or less stable $3R^2$ component. No transition from beidellite to montmorillonite is observed. Smectites from area 2 also plot in the "field" of fully expandable smectites but display a somewhat different trend. This trend is dominated by an increase in the $3R^2$ component as the composition moves from beidellitic to montmorillonitic up to a point beyond which the contribution of the $3R^2$ component remains constant. This behaviour is more obvious in sample SM66. Consequently, it seems that the transition from beidellite to montmorillonite exists only when Cheto-type montmorillonites are present.
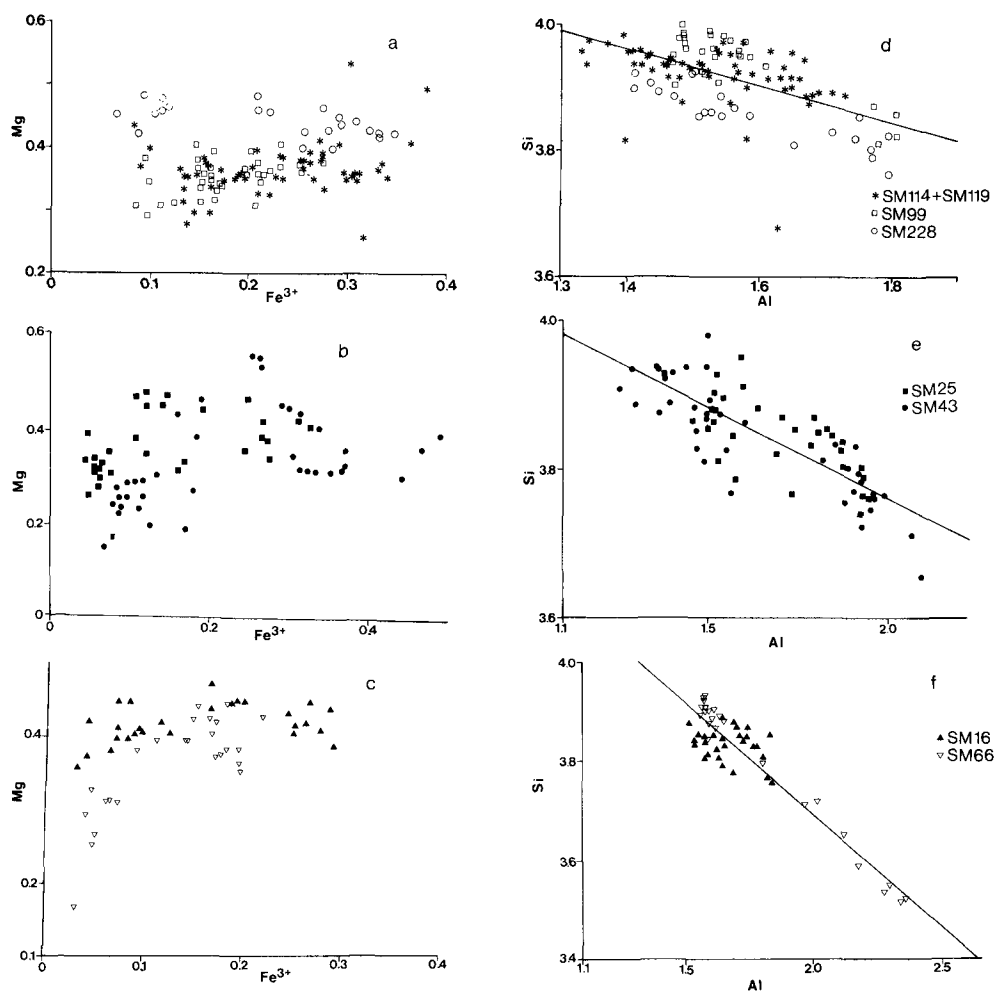
FIG. 5. Relationship between Mg and Fe^{3+} (a–c) and between Si and Al (d–f) in smectites. Note the well expressed negative relationship displayed by Si and Al. For discussion see text. Symbols for a, b and c are the same as for d, e and f.

DISCUSSION

Compositional variations in smectites

The wide variation in smectite composition among adjacent crystals confirms previous reports of heterogeneity of smectites and suggests that the average structural formulae do not provide sufficient indications about the range of variation of the smectite population in individual samples. The source for this heterogeneity is located in: (a) proportion of tetrahedral charge relative to octahedral charge, (b) variable substitutions in octahedral positions, (c) relative abundances of the exchangeable cations, and (d) variation of the total layer charge.

Although Cheto smectites from area 2 fulfil the compositional criteria necessary to be plotted in the appropriate "fields" of Güven's triangle, they do not comply with the layer charge criteria determined by Schultz (1969) but possess a low layer charge (Table 2).
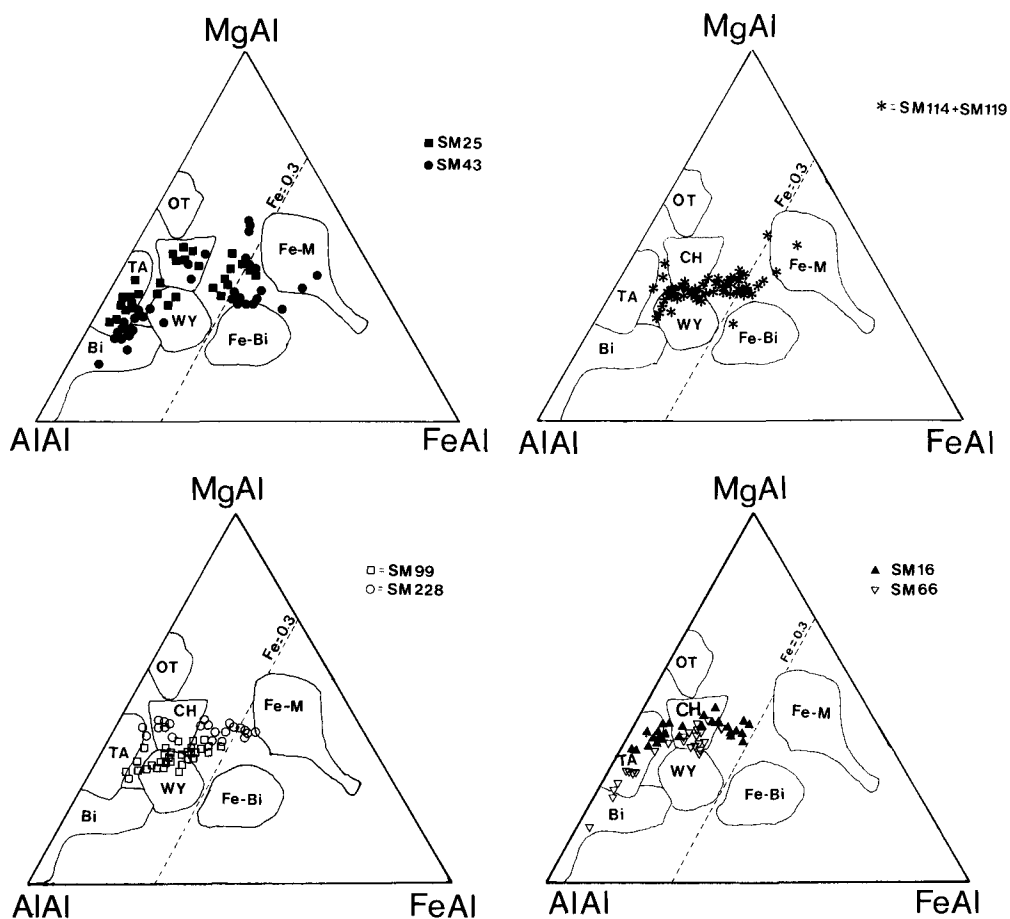
FIG. 6. Projection of the smectite compositions in the "smectite triangle" proposed by Güven (1988). Key to the different "smectite fields": OT = Otay montmorillonite; CH = Chambers montmorillonite; TA = Tatatilla montmorillonite; WY = Wyoming montmorillonite; Bi = Beidellite; Fe-Bi = Fe-rich beidellite; Fe-M = Fe-rich montmorillonite.

Possible reasons for this may be: (i) The assignment of the total number of Mg cations to octahedral sites. Christidis (1989) found that in smectites equivalent to those in SM228, Mg occupies nearly 50% of the exchangeable sites. This cannot be explained simply by hydrolytic extraction of Mg from the octahedral sheet. (ii) The assumption that octahedral Fe is present only in ferric state. The oxidation-reduction process is easily triggered, is reversible and is associated with structural changes in smectite (Stucki *et al.*, 1984; Lear & Stucki, 1985). It is possible, therefore that some iron is present in the ferrous state. Elzea & Murray (1990) reported smectites with Fe^{3+}/Fe^{2+} ratios as low as 0·05. (iii) Loss of exchangeable Na and/or K cations.

Implications for smectite formation

There is a well defined negative relationship between Al^{VI} and the other octahedral cations and between Si and total Al (Figs. 3–5) in all smectites analysed. In contrast, except
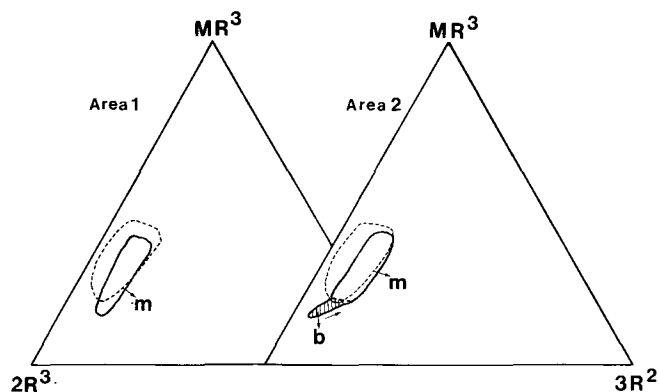
FIG. 7. Projection of the smectite compositions in the MR^3-$2R^3$-$3R^2$ triangle (Velde, 1985). (MR^3 = Na + K + 2Ca, $2R^3$ = (Al + Fe^{3+} − MR^3)/2, $3R^2$ = (Mg + Fe^{2+})/3). The arrow shows the compositional transition observed between beidellite and montmorillonite in the samples where the two minerals coexist. The area surrounded by the dashed line is occupied by natural fully expandable smectites (Velde, 1985). The area surrounded by the solid line corresponds to montmorillonites and the shaded area to beidellites of this study. m = montmorillonite. b = beidellite.

for SM228 (Area 1) in which definite trends, especially where Mg is involved, are observed, correlation between other octahedral cations, or between octahedral and tetrahedral cations, is lacking. This behaviour is believed to be relevant to the conditions which prevail during the formation of bentonites within small domains of the parent rock.

The parent rocks possibly had a dacitic–andesitic composition. Interaction of a glassy rock of such, or more, acidic composition with sea water, involves an initial ion exchange (White & Claasen, 1980; Shiraki & Iiyama, 1990), followed by diffusion through the depleted glass surface which is composed mainly of Si and Al (White & Claasen, 1980). Alkalis and Ca are easily released into the fluid phase, while Mg and $SO_4^=$ migrate to the host rock (Shiraki et al., 1987). The Mg content might increase up to 15 times during conversion of rhyolites to bentonite (Zielinski, 1982). Intermediate rocks have higher Mg content than rhyolites, which nevertheless is lower than that of smectites (Tables 2 and 3). Hence, some Mg might be added from sea water.

Because the Mg content of sea water reacting with the glass is constant, the variations in the Mg content of smectites might be due either to small-scale migration of the released Mg, or to different degrees of Mg uptake from the fluid phase in the different domains of the altered glass, or both. Hence, the fluid phase contributes to the variations in the Mg content. Small-scale migration is expected also for Fe. However, Fe^{2+} is mobile; it might be released into solution (Shiraki et al., 1987) and migrate for larger distances if oxygen fugacity is low, or it might be bound in smectite and/or iron oxides. Since Fe displays a near perfect negative relationship with Al, and Al is immobile under the conditions of bentonite formation (Zielinski, 1982; White 1983) it follows that (i) some Fe must be released from the original site, and (ii) this release is accompanied by a concomitant migration of Mg and/or Si (and/or differential selectivity of Mg from the fluid phase in the different domains) keeping the appropriate cation ratios.

In Fig. 8, Fe^{3+} and Al^{VI} are plotted with Si and Mg. The negative relationship displayed by Al^{VI} and Fe^{3+} is controlled by variations of both Si and Mg. The role of Mg is less well defined and in both areas two trends can be observed. In SM228 (area 1) it seems that the

control of Mg in the Fe for Al substitution is of major importance; smectites display the same trend as those from area 2 but not area 1, although they share the same precursor. In the other samples from area 1, the Fe for Al substitution is mainly controlled by the tetrahedral charge, since the Mg content is essentially constant over the total range of Al^{VI}/Fe^{3+} ratios. In beidellites (area 2) an increase in Mg is accompanied by an increase in the Fe content whereas in montmorillonites there is a decrease. Thus different chemical elements control the formation of different types of smectites.

The coexistence of beidellite with montmorillonite and/or montmorillonites with considerable variation in their tetrahedral charge, having Si/Al ratios lower than that of the parent glass, within distances not greater than 200–300 μm, indicates that the reaction rate controlling the release of Si is not of the same order in the various small domains of the parent rock. This might be due to microscale variations in the factors affecting the rate constant of the glass dissolution reaction i.e. pH of the solution (White, 1983), and/or fluid/ rock ratio (White & Claasen, 1980). Thus, the variability in chemistry and the physiochemical parameters of the microenvironment at the time of formation of smectites seem to be highly important for their compositional variations. The significance of the microenvironmental chemistry is also underlined by the fact that almost the same extent of chemical variation observed in individual samples characterizes the whole bentonite horizon from which they were taken (Figs. 3–5).

Two further alternatives for the compositional variations are addressed. The first assumes that the parent glass was inhomogeneous. It is difficult to assess this possibility because little is known about micro-scale variations in glass composition. The second assumes that the variation is a result of a mechanical mixture of particles.

Since each point analysed corresponds to a population of several smectite crystals, the chemical data obtained represent average chemical formulae of an unknown number of crystals. Hence, if only two distinct types of smectites are present in each analysed area, i.e. beidellite and montmorillonite, different proportions in the area analysed each time will

TABLE 3. Average chemical analyses (wt%) of intermediate rocks from Milos Island (from Fyticas, 1977).

|	Andesites poor in SiO_2	Andesites	Dacites
SiO_2	54·90	60·54	64·85
TiO_2	0·70	0·56	0·50
Al_2O_3	17·90	16·60	15·77
Fe_2O_3	3·75	3·19	2·65
FeO	3·35	2·11	1·75
MnO	0·10	0·14	0·10
MgO	4·05	3·23	2·22
CaO	9·30	6·85	5·42
Na_2O	3·15	3·46	3·65
K_2O	1·70	2·37	1·90
P_2O_5	0·07	0·14	0·07
H_2O^+	1·45	1·04	1·02
H_2O	–	–	–
Total	100·42	100·23	99·90
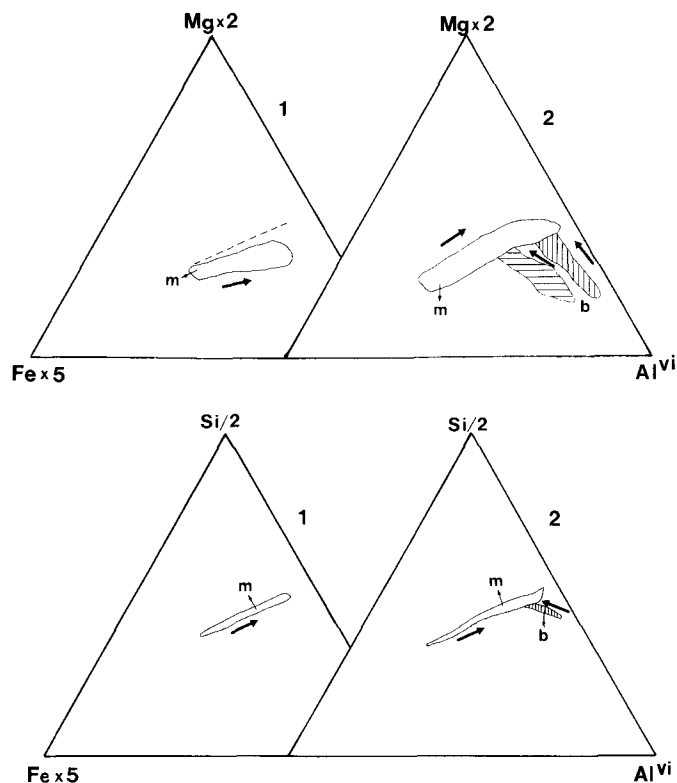
FIG. 8. Compositional trends shown by smectites examined in this study, given by the heavy arrows. 1 and 2 correspond to the areas 1 and 2 respectively, m corresponds to montmorillonite, and b to beidellite. The field covered by vertical hatching is occupied by beidellites from sample SM66 while that covered by horizontal hatching by beidellites from sample SM43. The dashed line shows the compositional trend exhibited by montmorillonites in the sample SM228 (area 1), which is very similar to that shown by montmorillonites of area 2. Note the different trend shown in beidellites, compared to montmorillonites. See text for discussion.

produce different average compositions. Had this been the case, then the smectites from area 2 in Fig. 6 would have displayed linear transitions between two poles. Instead, curvilinear trends are present, indicating that at least four chemically distinct end-members should be present. These end-members should combine in different ways with each other to obtain the Al^{VI}-Mg-Fe^{3+} ratios observed. This seems unlikely. Mechanical mixtures might account for variations in smectites with similar chemical characteristics.

Solid-solution series in smectites

The coexistence of Cheto-type smectites and beidellite with a range of compositions between them also indicates that the possibility of a solid-solution series between the two species cannot be ignored. Weaver & Pollard (1973) assumed a complete solid-solution between the two species, but Köster (1981) and Brigatti & Poppi (1981) considered that there is a miscibility gap between the two species. There is no particular reason to exclude the possibility of solid-solution at least between beidellite and Tatatilla-type montmoril-

lonite, which differ mainly in the distribution of the layer charge. The data in Fig. 6 display a clear range from a beidellitic to a montmorillonitic component through intermediate compositions, supporting the idea of solid-solution. However, because the transition between Tatatilla montmorillonite and beidellite is linear, the possibility of a mechanical mixture between a more Mg-rich and a more Al-rich component in different proportions cannnot be ignored. Detailed work with analytical electron microscopy is needed to clarify this point.

The fact that different types of montmorillonites having highly variable chemistry coexist within very small distances raises the question of solid-solution series among the montmorillonite species. Both series of smectites examined seem to converge chemically to a pole close to the Fe montmorillonite "field". However, there does not seem to be any transition between montmorillonites plotted in the "fields" assigned to Chambers or Tatatilla and Wyoming types. This indicates a miscibility gap between Cheto and Wyoming montmorillonites in accordance with the assumption of Grim & Kulbicki (1961). Nevertheless, the fact that a great number of points from both series plot in an area not assigned to any particular field means that the field boundaries need reconstruction. With the existing data the "common field" cannot be resolved with certainty. Consequently, the possibility of a solid-solution series between Cheto montmorillonites and Fe-rich Wyoming montmorillonites cannot be rejected.

It is not clear why a transition from beidellite to Wyoming montmorillonite has not been observed. A possible explanation is that the higher amount of Fe and the lower layer charge present in Wyoming-type montmorillonites requires more complicated structural re-arrangements to obtain a solid-solution series. This is indicated from the different substitution pattern Al^{VI}-Fe^{3+}-Mg between Wyoming and Cheto montmorillonites (Fig. 8). Also, it seems that in the samples where both smectites coexist (especially in SM66) the transition between beidellite-Tatatilla montmorillonite and Tatatilla-Chambers montmorillonite is questionable. Although this might be due to the relatively small number of microanalyses, the incompatibility of Mg and Fe in the structure of both beidellite and Tatatilla montmorillonite should not be excluded.

REFERENCES

ALBERTI A. & BRIGATTI M.F. (1985) Crystal chemical differences in Al-rich smectites as shown by multivariate analysis of variance and discriminant analysis. *Clays Clay Miner.* **33**, 546–558.

ALTANER S.P. & GRIM R.E. (1990) Mineralogy, chemistry and diagenesis of tuffs in the Sucker Creek formation (Miocene), Eastern Oregon. *Clays Clay Miner.* **38**, 561–572.

ALTHERR R., SCHLIESTEDT M., OKRUSCH M., SEIDEL E., KREUZER H., HARRE W., LENZ H., WENDT I. & WAGNER G.A. (1979) Geochronology of high-pressure rocks on Siphnos (Cyclades, Greece). *Contrib. Mineral. Petrol.* **70**, 245–255.

ANGELIER J., CANTAGREL J.-M. & VILMINOT J.-C. (1977) Neotectonique cassante et volcanisme plio-quaternaire dans l'arc egeen interne: l'isle de Milos (Grece). *Bull. Soc. geol. France (7). t.XIX*, **1**, 119–123.

BANFIELD J.F. & EGGLETON R.A. (1990) Analytical transmission electron microscope studies of plagioclase, muscovite, and K-feldspar weathering. *Clays Clay Miner.* **38**, 77–89.

BOUCHET A., PROUST D., MEUNIER A. & BEAUFORT D. (1988) High-charge to low-charge smectite reaction in hydrothermal alteration processes. *Clay Miner.* **23**, 133–146.

BRIGATTI M.F. & POPPI L. (1981) A mathematical model to distinguish the members of the dioctahedral smectite series. *Clay Miner.* **16**, 81–89.

BYRNE P.J.S. (1954) Some observations on montmorillonite-organic complexes. *Clays Clay Miner.* **2**, 241–253.

CHRISTIDIS G. (1989) *Mineralogy, physical and chemical properties of the bentonite deposits of Milos island, Greece.* MSc thesis, Univ. Hull, UK.

DUNHAM A.C. & WILKINSON F.C.F. (1978) Accuracy, precision and detection limits of energy dispersive electron-microprobe analyses of silicates. *X-ray Spectrometry* **7**, 50–56.

ELIZEA J.M. & MURRAY H.H. (1990) Variation in the mineralogical, chemical and physical properties of the Cretaceous Clay Spur bentonite in Wyoming and Montana. *Appl. Clay Sci.* **5**, 229–248.

FYTICAS M., GIULLIANI O., INNOCENTI F., MARINELLI G. & MAZZUOLI R. (1976) Geochronological data on recent magmatism of the Aegean Sea. *Tectonophysics* **31**, T29–T34.

FYTICAS M. (1977) *Geological and geothermal study of Milos island.* PhD thesis, Univ. Salonica, Greece.

FYTICAS M., INNOCENTI F., KOLIOS N., MANETTI P., MAZZUOLI R., POLI G., RITA F. & VILLARI L. (1986) Volcanology and petrology of volcanic products from the island of Milos and neighbouring islets. *J. Volcanol. Geotherm. Res.* **28**, 297–317.

GOODMAN B.A., NADEAU P.H. & CHADWICK J. (1988) Evidence for the multiphase nature of bentonites from Mössbauer and EPR spectroscopy. *Clay Miner.* **23**, 147–159.

GOULDING K.W.T. & TALIBUDEEN O. (1980) Heterogeneity of cation-exchange sites for K-Ca exchange in aluminosilicates. *J. Coll. Interf. Sci.* **78**, 15–24.

GRIM R.E. & KULBICKI G. (1961) Montmorillonite: High temperature reactions and classification. *Am. Miner.* **46**, 1329–1369.

GRIM R.E. & GÜVEN N. (1978) *Bentonites. Geology, Mineralogy, Properties and Uses.* pp. 143–155. Elsevier, Amsterdam.

GÜVEN N. (1988) Smectite. Pp. 497–559 in: *Hydrous Phyllosilicates (Exclusive of Micas)* (S.W. Bailey, editor). Reviews in Mineralogy, vol. **19**. Mineralogical Society of America, Washington, DC.

HOFFMANN C. & KELLER J. (1979) Xenoliths of lawsonite-ferroglaucophane rocks from a Quaternary volcano of Milos (Aegean Sea, Greece). *Lithos* **12**, 209–219.

KÖSTER H.M. (1981) The crystal structure of 2:1 layer silicates. *Proc. Int. Clay Conf. Pavia-Bologna,* 41–71.

KORNPROBST J., KIENAST J.-R. & VILMINOT J.-C. (1979) The high-pressure assemblages at Milos, Greece. *Contrib. Mineral. Petrol.* **69**, 49–63.

LAGALY G. (1981) Characterization of clays by organic compounds. *Clay Miner.* **16**, 1–21.

LAGALY G. & WEISS A. (1975) The layer charge of smectitic layer silicates. *Proc. Int. Clay Conf. Mexico,* 157–172.

LAGALY G., FERNANDEZ-GONZALEZ M. & WEISS A. (1976) Problems in layer-charge determination of montmorillonites. *Clay Miner.* **11**, 173–187.

LEAR P.R. & STUCKI J.W. (1985) Role of structural hydrogen in the reduction and re-oxidation of iron in nontronite. *Clays Clay Miner.* **33**, 539–545.

LIM C.H. & JACKSON M.L. (1986) Expandable phyllosilicate reactions with lithium on heating. *Clays Clay Miner.* **34**, 346–352.

LUTTIG G. & WIEDENBEIN F. (1990) Bentonite and related deposits. World economic significance and situation in Greece. *Abstracts 5th Congr. Geol. Soc. Greece, Thessaloniki.*

MCATEE J.L. (1958a) Heterogeneity in montmorillonite. *Clays Clay Miner.* **5**, 279–288.

MCATEE J.L. (1958b) Random interstratification in organophilic bentonites. *Clays Clay Miner.* **5**, 308–317.

NADEAU P.H., FARMER V.C., MCHARDY W.J. & BAIN D.C. (1985) Compositional variations of the Unterrupsroth beidellite. *Am. Miner.* **70**, 1004–1010.

NEWMAN A.C.D. & BROWN G. (1987) The chemical constitution of clays. Pp. 1–128 in: *Chemistry of Clays and Clay Minerals* (A.C.D. Newman, editor). Mineralogical Society, London.

NORRISH K. (1954) The swelling of montmorillonite. *Disc. Faraday Soc.* **18**, 120–134.

RAMSEYER K. & BOLES J.R. (1986) Mixed-layer illite/smectite minerals in Tertiary sandstones and shales, San Joaquin Basin, California. *Clays Clay Miner.* **34**, 115–124.

SCHULTZ L.G. (1969) Lithium and potassium adsorption, dehydroxylation temperature and structural water content of aluminous smectites. *Clays Clay Miner.* **17**, 115–149.

SHIRAKI R., SAKAI H., ENDOH M. & KISHIMA N. (1987) Experimental studies on rhyolite-and andesite-seawater interactions at 300°C and 1000 bars. *Geochemical J.* **21**, 139–148.

SHIRAKI R. & IIYAMA T. (1990) Na-K ion exchange reaction between rhyolitic glass and (Na,K)Cl aqueous solution under hydrothermal conditions. *Geochim. Cosmochim. Acta* **54**, 2923–2931.

SINGH BALWANT & GILKES R.J. (1991) A potassium-rich beidellite from a laterite pallid zone in Western Australia. *Clay Miner.* **26**, 233–244.

SONDER R.A. (1924/25) Zur Geologie und Petrographie der Inselgruppe von Milos. *Z. Volcanologie* **8**, 181–237.

STUCKI J.W., LOW P.F., ROTH C.B. & GOLDEN D.C. (1984) Effects of oxidation state of octahedral iron on clay swelling. *Clays Clay Miner.* **32**, 357–362.

STUL M.S. & MORTIER W.J. (1974) The heterogeneity of the charge density in montmorillonites. *Clays Clay Miner.* **22**, 391–396.

TALIBUDEEN O. & GOULDING K.W.T. (1983) Charge heterogeneity in smectites. *Clays Clay Miner.* **31**, 37–42.

TETTENHORST R. & JOHNS W.D. (1966) Interstratification in montmorillonite. *Clays Clay Miner.* **25**, 85–93.

VELDE B. (1984) Electron microprobe analysis of clay minerals. *Clay Miner.* **19**, 243–247.

VELDE B. (1985) *Clay Minerals. A Physico-Chemical Explanation of their Occurrence,* pp. 38–43 and 104–145. Elsevier, Amsterdam.

WEAVER C.E. & POLLARD L.D. (1973) *The Chemistry of Clay Minerals,* pp. 55–77. Elsevier, Amsterdam.

WETZENSTEIN W. (1969) *Die Bentonitlagerstatten im Osteil der Insel Milos/Griechenland und ihre mineralogische Zussamensetzung.* PhD thesis, Univ. Stuttgart, Germany.

WETZENSTEIN W. (1972) Die Bentonitlagerstatten im Osteil der Insel Milos und ihre mineralogische Zussamensetzung. *Bull. Geol. Soc. Greece* **9**, 144–171.

WHITE A.F. & CLAASEN H.C. (1980) Kinetic model for the short term dissolution of a rhyolitic glass. *Chem. Geol.* **28**, 91–109.

WHITE A.F. (1983) Surface chemistry and dissolution kinetics of glassy rocks at 25°C. *Geochim. Cosmochim. Acta* **47**, 805–815.

WRIGHT T.L. (1968) X-ray and optical study of alkali-feldspar: II. An X-ray method for determining the composition and structural state from measurement of 2θ values for three reflections. *Am. Miner.* **53**, 88–104.

YAMADA H., NAKAZAWA H., YOSHIOKA K. & FUJITA T. (1991) Smectites in the montmorillonite-beidellite series. *Clay Miner.* **26**, 359–369.

ZIELINSKI R.A. (1982) The mobility of uranium and other elements during alteration of rhyolite ash to montmorillonite: A case study in the Troublesome Formation, Colorado, USA. *Chem. Geol.* **35**, 185–204.